

Dynamic CTCF binding directly mediates interactions among *cis*-regulatory elements essential for hematopoiesis

Qian Qi^{1#}, Li Cheng^{1#}, Xing Tang¹, Yanghua He¹, Yichao Li¹, Tiffany Yee¹, Dewan Shrestha¹, Ruopeng Feng¹, Peng Xu¹, Xin Zhou², Shondra Pruett-Miller³, Ross C. Hardison⁴, Mitchell J. Weiss¹, Yong Cheng^{1,2*}

1. Department of Hematology, St. Jude Children's Research Hospital, Memphis, TN 38105, USA
2. Department of Computational Biology, St. Jude Children's Research Hospital, Memphis, TN 38105, USA
3. Center for Advanced Genome Engineering, St. Jude Children's Research Hospital, Memphis, TN 38105, USA
4. Department of Biochemistry and Molecular Biology, Pennsylvania State University, University Park, PA 16802, USA.

*Correspondence:

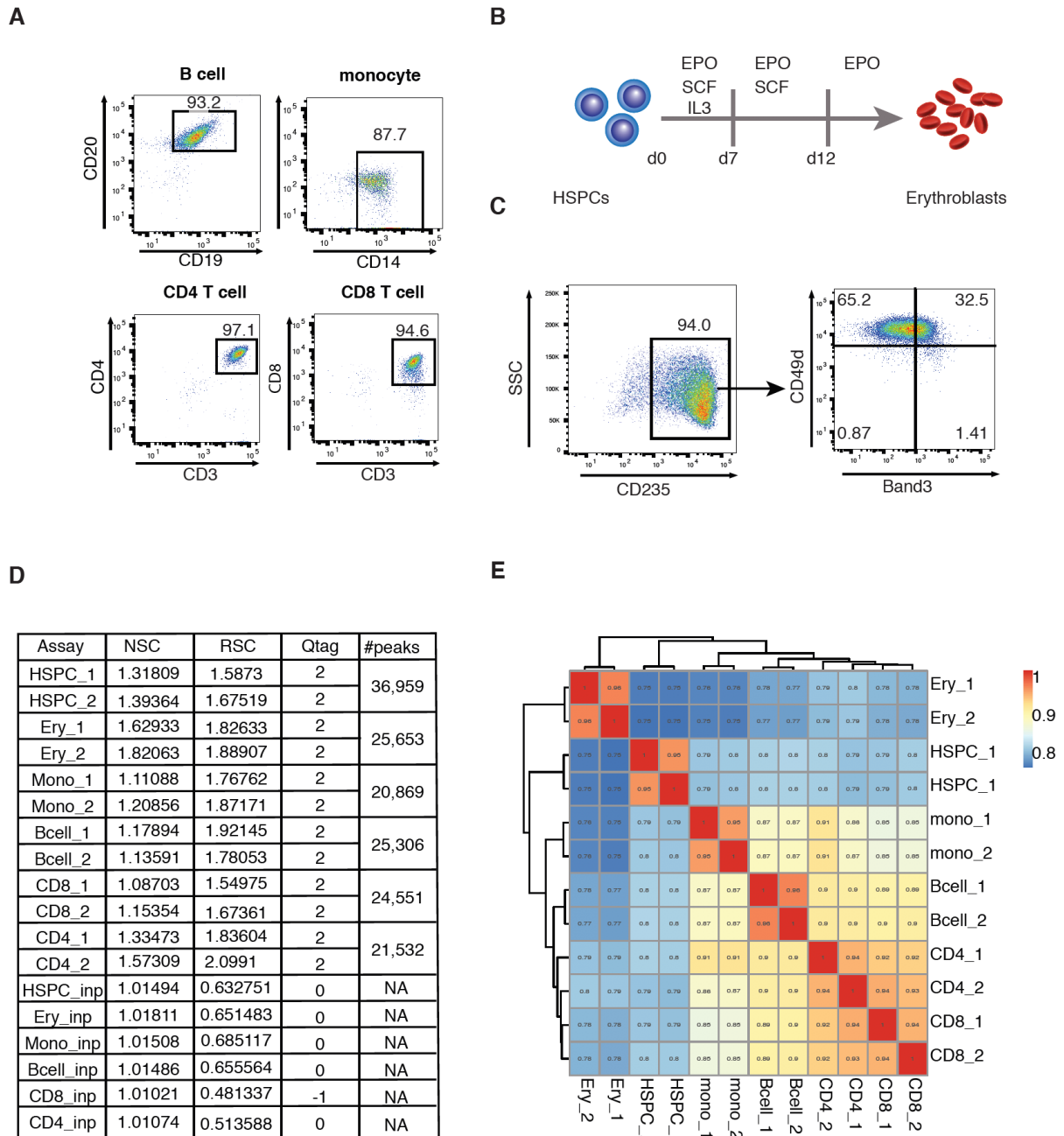
Yong Cheng, PhD
St. Jude Children's Research Hospital
262 Danny Thomas Place, MS-355
Memphis, TN 38105
yong.cheng@stjude.org

equal contribution

Supplementary Material

Supplementary Figures

Figure S1

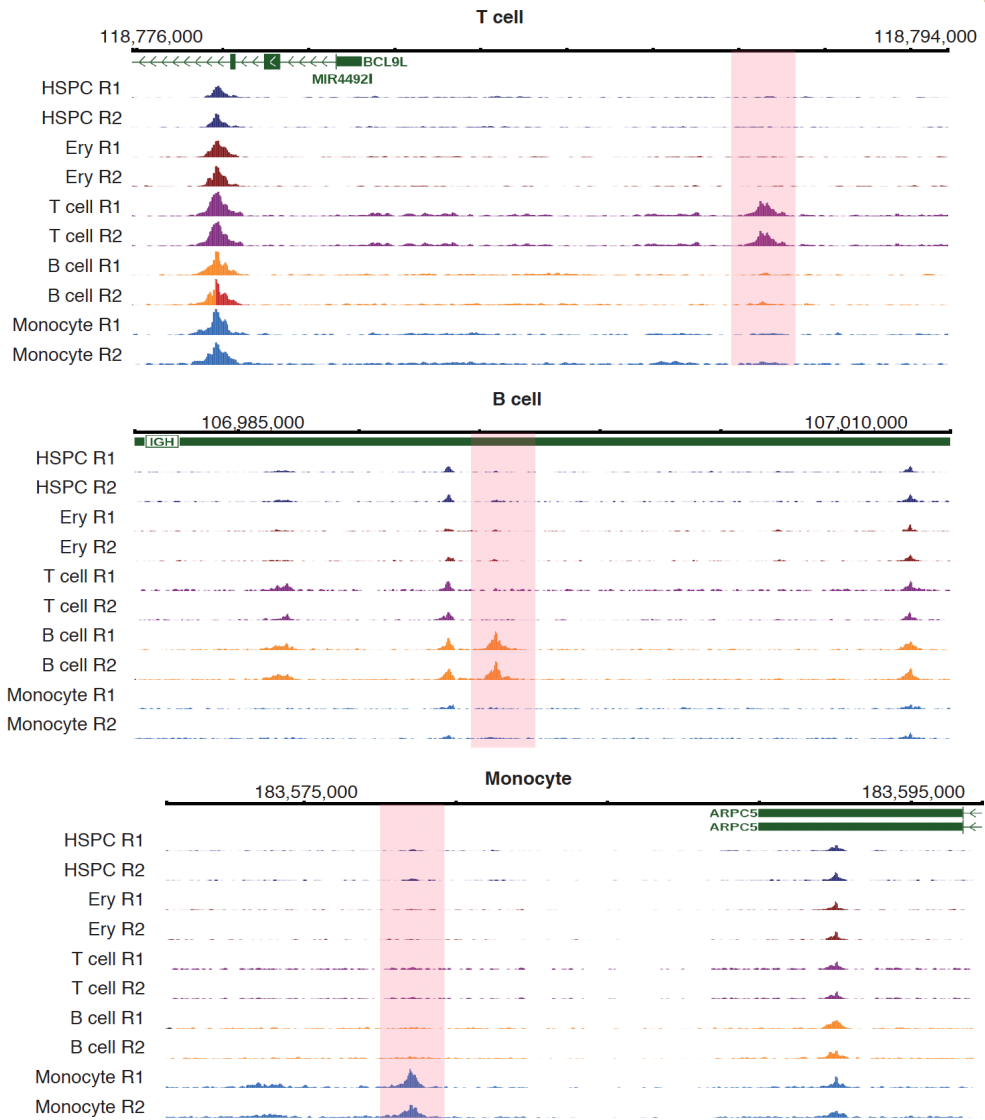


Supplementary Fig.1. A, B cells, monocytes, CD4⁺ T cells, and CD8⁺ T cells were isolated from CD34⁻ PBMCs with their corresponding microbeads. Flow cytometric plots

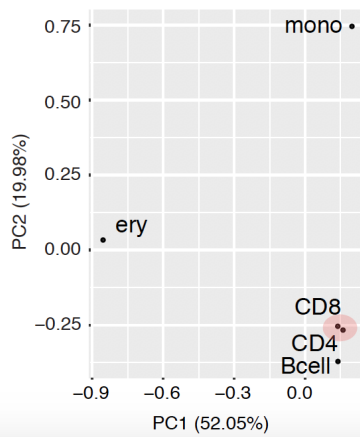
show the purity of B cells, monocytes, CD4⁺ T cells, and CD8⁺ T cells were 93.2%, 87.7%, 97.1%, and 94.6%, respectively. **B**, The 3-phase in vitro erythropoiesis protocol for human HSPCs. **C**, Flow cytometric plots of erythroid marker CD235a (glycophorin A) levels after CD34⁺ HSPCs were maintained in erythroid differentiation medium for 12 d (left panel). The levels of Band3 and CD49d in the gated CD235a⁺ cells were measured by flow cytometry (right panel). **D**, ChIP-seq quality measured by Cross-correlation analysis and total number of peaks detected. **E**, Heatmap showing the unsupervised hierarchical clusters based on Pearson correlation of CTCF ChIP-seq signals in different blood cell lineages. Numbers represent the value of Pearson correlation coefficient.

Figure S2

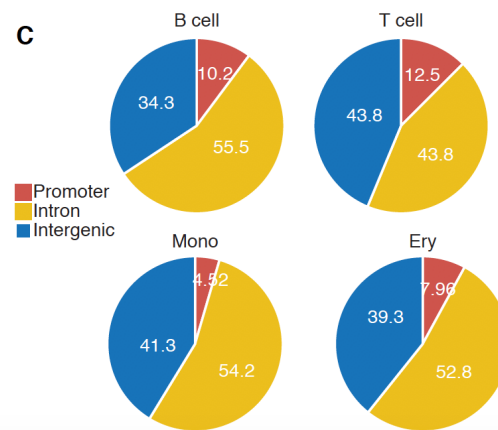
A



B

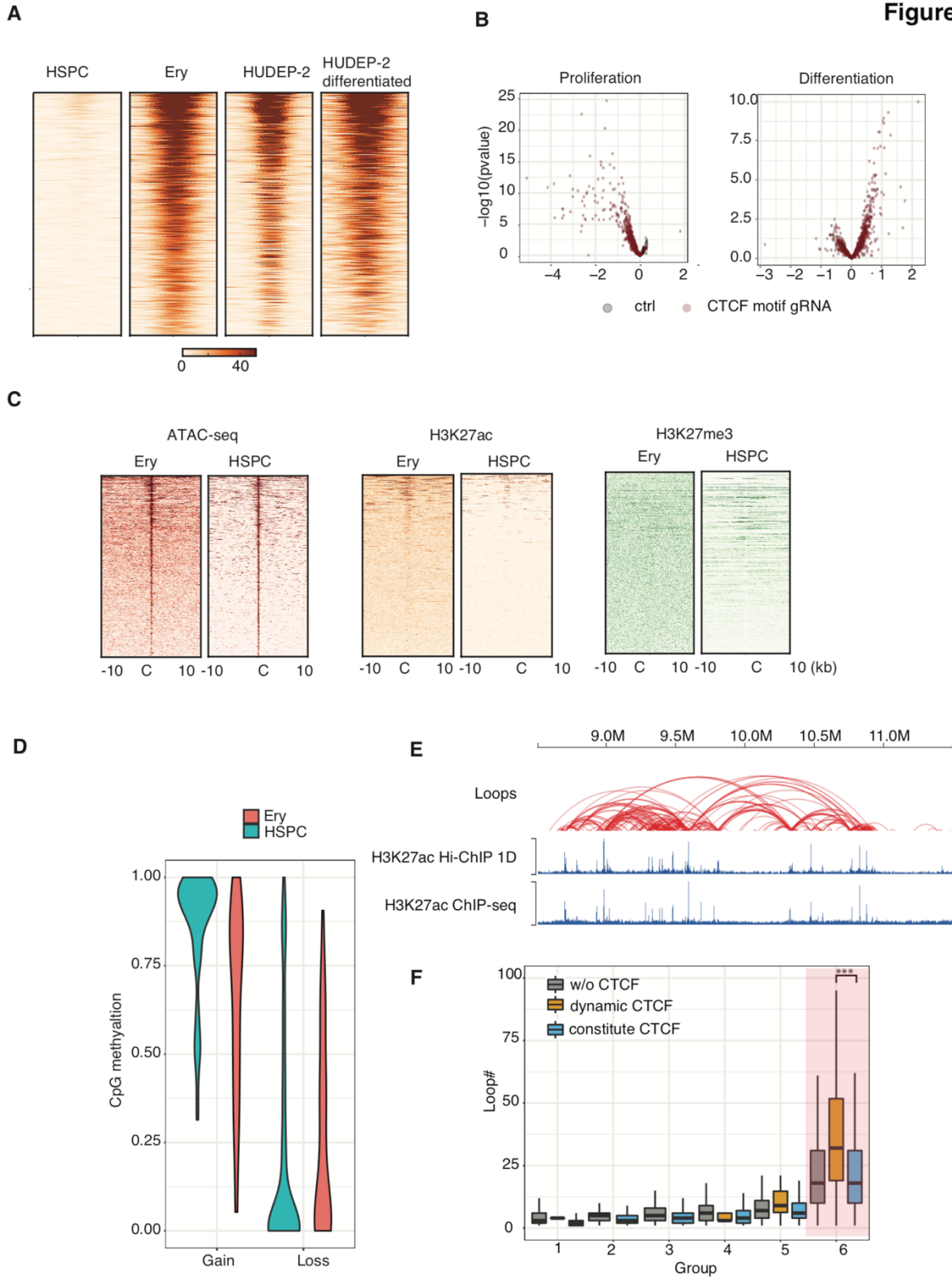


C



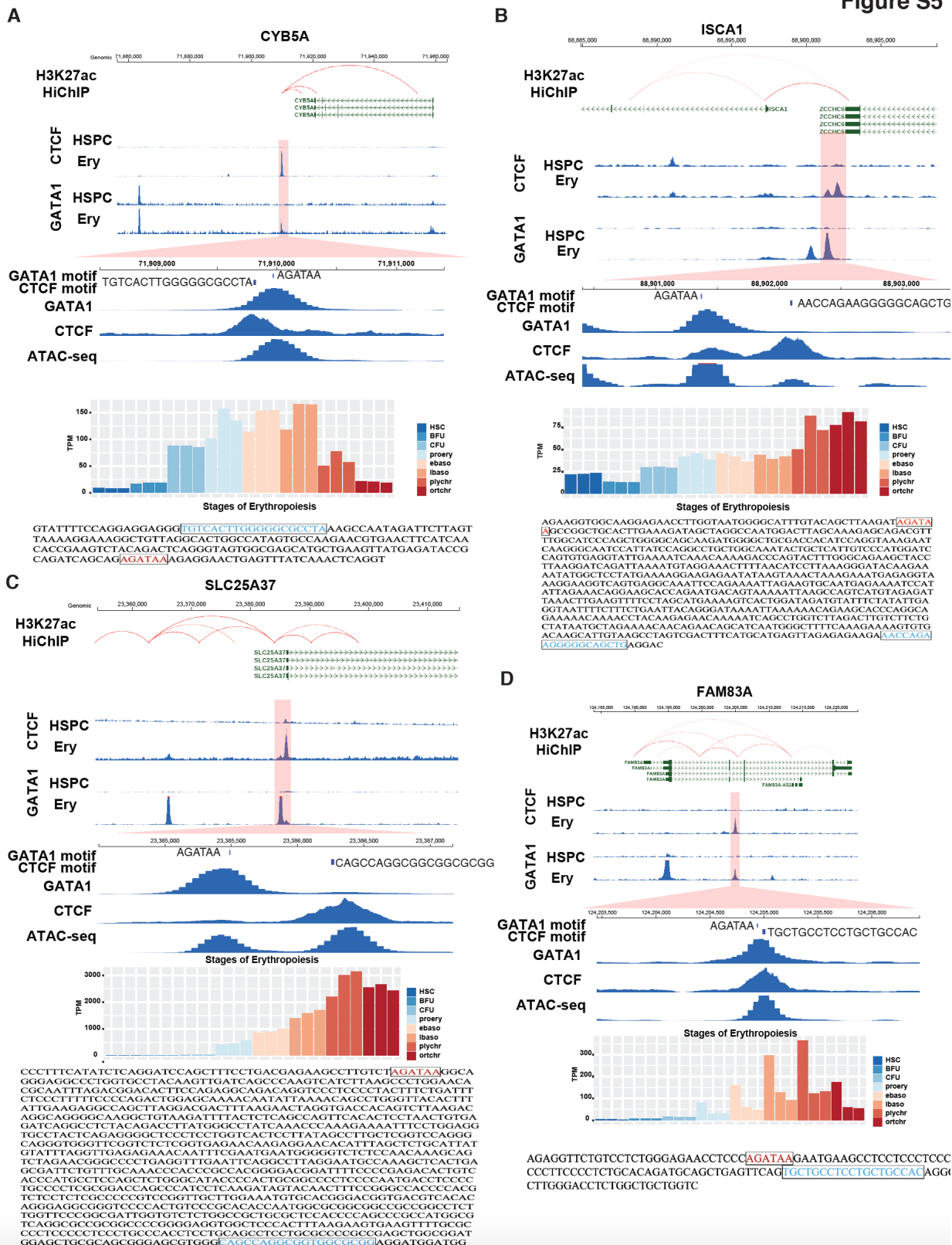
Supplementary Fig. 2. A, Genome browser tracks showing dynamic CTCF-binding sites (highlighted in pink) in T cell, B cell, and Monocyte respectively. **B**, PCA analysis of CTCF ChIP-seq in different blood lineages. The PCA is based on the raw ChIP-seq signal at CTCF binding sites. **C**, Pie charts showing percent of dynamic CTCF sites in different genomic locations. Promoters are defined as +/-2000bp of transcription start sites (TSSs).

based on absolute value. **D**, GWAS hits enrichment analysis were conducted using randomly (100X) selected GATA1 and PU.1 peaks in erythroid and B-cells that have the same total numbers and length distribution as the dynamic CTCF sites. If the q-value of the dynamic CTCF sites was more significant than all the 100 random ones, the rank was 1st. In contrast, if the q-value was less significant than the 100 random ones, the rank was 100th. The actual ranking of dynamic CTCF sites for each trait is plotted.

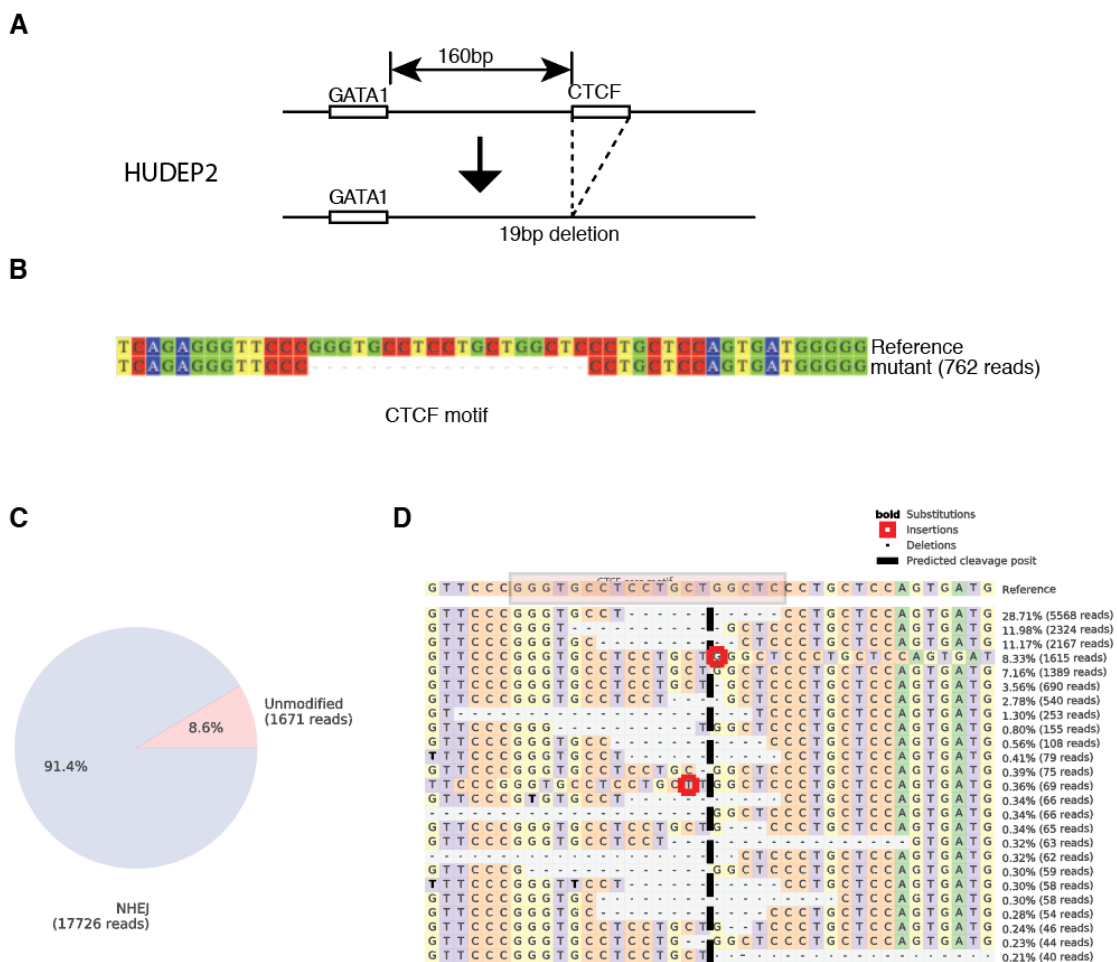
Figure S

Supplementary Fig. 4. A, Heatmap represents the ChIP-seq signals distribution of 378 erythroid dynamic CTCF sites within (+/- 500bp window) centered by the ChIP-seq peaks. **B,** Cas9-expressing HUDEP-2 cells were transduced with a lentiviral vector library containing 1188 sgRNA targeting erythroid dynamic CTCF-binding sites and 100 control nontarget sgRNAs. Left panel: A volcano plot is depicted with the log₂ fold change for each gRNA between cells that grow in expansion medium on 0 and 8 days. Right panel: A volcano plot is depicted with the log₂ fold change for each sgRNA between Band3⁺ and Band3⁻ cells after 5 days of induced erythroid maturation. **C,** Heatmap showing the signals of ATAC-seq, H3K27ac, and H3K27me3 ChIP-seq near the 20-kb windows of constitutive CTCF-binding sites in HSPCs and erythroblasts. **D,** Violin box plots showing the CpG methylation levels of GOSs and LOSs in HSPCs and erythroblasts. **E,** Screenshot of loops identified by H3K27ac HiChIP (top), H3K27ac HiChIP signal (middle), and H3K27ac ChIP signal tracks (bottom) in CD34⁺ HSPCs derived erythroblasts from the same donor in a 3-Mb window. **F,** Each boxplot represents the distribution of the number of loops per anchor region (y-axis). The different groups of loop-anchors based on the enrichment of H3K27ac signals from low (group 1) to high (group 6) are presented on the x-axis. *** marks the comparison with a significant difference (p-value < 2.2e-16) in the number of loops per anchor between dynamic CTCF sites and constitute CTCF sites in group 6 (highlighted), using a Wilcoxon-test.

Figure S5



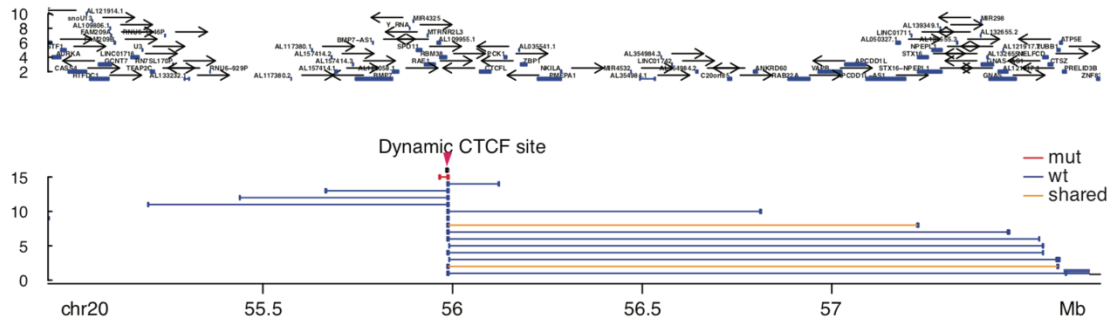
Supplementary Fig. 5. Examples of dynamic CTCF sites co-localized with GATA1 peaks and implicated in regulating gene expression during erythropoiesis. Within each locus, the top panel is the screenshot of genome browser that includes the CRE-loops detected by H3K27ac HiChIP, CTCF and GATA1 ChIP-seq in HSPC and erythroid cells. The middle panel shows a zoomed-in view (highlighted in Pink) of the peaks and consensus motifs of GATA1 and CTCF together with ATAC-seq signals in erythroid cells. The bottom panel shows the expression level (RNA-seq) of each gene at different stages of hematopoiesis. DNA sequences around CTCF and GATA1 motifs are shown in the bottom panel with motif sequences highlighted and boxed.



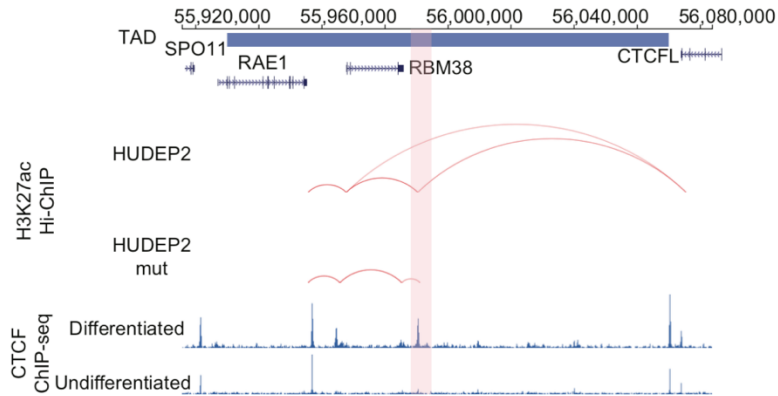
Supplementary Fig. 6. A, Schematic of the CTCF-binding motif near the *RBM38* gene deleted with homology-directed genome editing in HUDEP-2 cells. A GATA1 binding site is located 160-bp upstream of this CTCF-binding motif. **B**, Alignment of targeted deep sequencing data in a homozygous mut HUDEP-2 clone with the CTCF motif deleted. **C–D**, A Cas9 RNP with a gRNA targeting the CTCF motif was transiently transfected in CD34⁺ HSPCs. HSPCs were grown in the erythroid Phase I differentiation medium for 7 d and then harvested for targeted deep sequencing. (C) Pie chart showing the percentage of modified (purple) and unmodified DNA sequences. (D) Alignment of targeted deep-sequencing data.

Figure S7

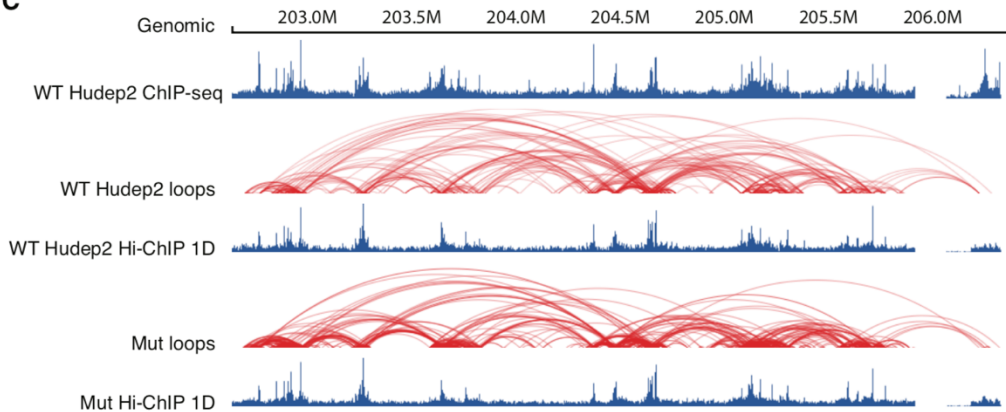
A



B



C



Supplementary Fig. 7. A. Top panel shows the location and transcriptional direction of genes. The bottom panel represents the interactions involved with the dynamic CTCF-binding site measured by H3K27ac HiChIP in CD34⁺ HSPCs differentiated erythroblasts. The color represents the different types of interactions. Blue, interactions in wildtype HUDEP2 cells only, orange, interactions shared between wildtype and mutant cells. Red, interactions in mutant cells only. **B,** Screenshot of chromatin interactions and related ChIP-seq signals within the TAD containing *RBM38* gene. The dynamic CTCF binding site is highlighted. **C,** Screenshot of 3D chromatin loops and ChIP-seq signals identified by H3K27ac-HiChIP with WT HUDEP-2 cells and a mut clone after 3 days of induced maturation.

Supplementary Table Legends (separate files)

Supplementary Table 1. List of dynamic CTCF sites in Erythroid cells, B cells, T cells and Monocytes. The coordinates and summits of the peaks; Log2 fold change, p-value and adjust p-value of Deseq2; the ChIP-seq signals and existence of TF motifs within +/-200bp of peak summits; the nearest gene and distance, together with the 3D interactions of promoters detected by promoter capture Hi-C and HiChIP against H3K27ac are shown.

Supplementary Table 2. DNA oligo sequences targeting RBM38 promoter for capture Hi-C. Two DNA sequences of biotinylated oligos used are shown.

Supplementary Table 3. List of functional genomic data used in this study. The cell type, culture condition, antibodies of newly generated are shown. The access ID of downloaded data are shown.